Dynamics of the OH + Cl_2 → HOCl + Cl Reaction: Ab Initio Investigation and Quasiclassical Trajectory Calculations of Reaction Selectivity

Vasilios S. Melissas,[†] Evangelos Drougas,[‡] Evangelos G. Bakalbassis,[§] and Agnie M. Kosmas*[,‡]

Molecular Modelling of Materials Laboratory, Institute of Physical Chemistry, NRCPS "Demokritos", 153 10 Agia Paraskevi Attikis, Greece, Laboratory of Physical Chemistry, Department of Chemistry, University of Ioannina, 451 10 Ioannina, Greece, and Laboratory of Applied Quantum Chemistry, Department of Chemistry, Aristotle University of Thessaloniki, P.O. Box 135, 540 06 Thessaloniki, Greece

Received: August 10, 1999; In Final Form: November 1, 1999

The selectivity of reactant rotational and vibrational energy upon reactive cross sections for the reaction OH + Cl_2 → HOCl + Cl is investigated in detail by performing quasiclassical trajectory (QCT) calculations on a six-dimensional, analytically constructed potential energy surface (PES). The construction of the PES was based on ab initio molecular orbital calculations of the HOClCl system using the unrestricted second-order Møller−Plesset perturbation theory approach. The quantum mechanical investigation produced three stationary points relevant to the title reaction, a transition-state configuration and two HOCl···Cl-type complexes. Geometries, energies, and vibrational frequencies are reported for these structures. The analytical functional form for the PES has been developed following the Schatz−Elgersma formulation incorporating the Sorbie−Murrell potential energy term for the HOCl molecule. Extended three-dimensional QCT calculations at low and moderate collision energies covered several rotational and vibrational reactant states to produce a detailed study of the selectivity upon the reactivity of the system. The resulting dynamical features are the strong enhancement of reactivity when the vibrational content of the breaking bond is raised and the exactly opposite effect when the vibrational excitation of the spectator OH bond is increased. The initial reactant rotation is shown to have a very minor influence on the dynamics.

Introduction

Several recent experimental and theoretical studies have produced interesting details concerning the dynamics and kinetics of various gas-phase elementary four-atom reactions.[1−8] An important class of such systems are the reactions of hydroxyl radical with halogen and interhalogen molecules which have been well characterized experimentally[9−18] but have received much less attention concerning their dynamical investigation.

The reaction between the hydroxyl radical and the chlorine molecule has been extensively studied experimentally by Loewenstein and Anderson[14] at 298 K and by Wayne and co-workers,[15] who made an investigation of the reaction from 253 to 333 K. The reaction presents a low endothermicity at room temperature between 7.53 and 4.31 kJ/mol, and the corresponding experimental rate coefficients at 298 K reported by these workers are $(6.70 \pm 0.72) \times 10^{-14}$ and $(6.8 \pm 1.0) \times 10^{-14}$ cm^3 $molecule^{-1}$ s^{-1}, respectively. Other experimental measurements range from $(5.5 \pm 0.3) \times 10^{-14}$ cm^3 $molecule^{-1}$ s^{-1} [10] to 7.4×10^{-14} cm^3 $molecule^{-1}$ s^{-1},[11] values within 20% of the former quoted ones. Loewenstein and Anderson also measured at room temperature the branching ratio to the HCl + ClO channel that is exothermic by 38.1 kJ/mol. This branching ratio was found negligible, and the reaction proceeds practically to the breaking of the Cl−Cl bond and the formation of the HOCl molecule also consistent with the studies for the reverse reaction HOCl + Cl that was recognized to lead to OH + Cl_2 products.[19] Consequently, the title reaction represents a nice system to test the role of the nonbreaking OH bond in the dynamics of another diatom−diatom reaction. From the mechanistic point of view the experimental kinetic studies were consistent with the assumption that the reaction proceeds through the formation of a short-lived collision complex in analogy with the dynamical behavior observed for OD + ICl and OD, OH + Br_2 reactions.[16,18]

In a recent study[20] we have made a first dynamical investigation of the title reaction based on two model potential energy surfaces. The methodology followed was based on the two most commonly encountered procedures in the literature, the formulation suggested by Bowman and co-workers[21] and the one by Elgesma and Schatz.[22] Both of these functional forms with important improvements[23] in several cases have been the starting points in the construction of the potential energy surface (PES) for the dynamical study of most four-atom systems. Our two model PESs so constructed were designed to incorporate similar values for the entrance barrier based on the experimental activation energy, i.e., around 7.5 kJ mol^{-1}, and they both contained a potential energy well consistent with the experimental evidence and the dynamical behavior of similar systems. However, in the absence of any ab initio information the potential energy minima were designed to differ substantially, ranging from 8.6 kJ mol^{-1} in the first surface to 40.1 kJ mol^{-1} in the second, thus covering a wide area of possible values with the hope that the true energy minimum would be located somewhere between. This study has given a qualitative picture of the mechanism of the reaction and has revealed several interesting dynamical features such as the severe increase of the reactive cross section with collision energy and the spectator role of the nonbreaking OH bond, regardless of the magnitude

* Corresponding author.
[†] NRCPS "Demokritos".
[‡] University of Ioannina.
[§] University of Thessaloniki.

10.1021/jp9928098 CCC: $19.00
Published on Web 12/31/1999

of the potential well. However, the uncertainty in the detailed parameters of the PES has resulted in large discrepancies in the quantitative dependence of the cross section on collision energy between the two PESs and the inability to properly investigate the role of the reactant internal energy.

With the increasing feasibility of high-quality quantum mechanical calculations, the major obstacle in studying the dynamics of four and more atom reactions, i.e., the lack of reliable ab initio molecular electronic structure data, has definitely been overcome. Lately, several theoretical calculations for chlorine molecule containing van der Waals complexes have been reported in the literature.[24,25] For the present system no ab initio calculations have been carried out yet, but an extensive quantum mechanical study has been published recently for two systems, the Cl_2···ClO and HCl···ClO complexes[26] which are closely related to the title reaction. Consequently, a quantum mechanical study of the $HOCl_2$ system was considered necessary to construct an analytical PES that can be trusted to describe quantitatively the mechanism of the reaction. Molecular orbital calculations have been performed at the unrestricted second-order Møller−Plesset (UMP2) level of theory[27] using the 6-31G-(d), 6-311++G(d, p), and correlation-consistent polarized-valence double- and triple-ζ (cc-pVnZ) basis sets. On the basis of the quantum calculations, our previously constructed Elgesma and Schatz type PES, being closer to the ab initio findings, was employed after minor modifications to perform detailed quasiclassical trajectory (QCT) calculations which allowed a more faithful description of the dynamics of the reaction.

Quantum Calculations and Results

The quantum mechanical investigation of the OH + Cl_2 surface was carried out by using the unrestricted second-order Møller−Plesset perturbation theory[27] with the Gaussian 94 code[28] employed throughout the calculations. As the first step the accuracy of our MP2 procedure was tested by examining the HCl···ClO complex at the UMP2/6-31G(d) level of theory, already studied.[26] As mentioned previously, an extensive ab initio molecular orbital study of systems related to the title reaction has been recently reported, i.e., the theoretical study of Cl_2−ClO and HCl−ClO complexes.[26] Of these systems the former one was found to present two minimum-energy van der Waals structures, one bonded via the oxygen end of the chlorine oxide and a second one bonded via the chlorine atom on the same molecule. The latter system HCl−ClO was determined to assume a hydrogen-bonded structure with three nearly collinear atoms ClH···O and the fourth, the chlorine atom of the ClO molecule, forming an angle with the line. Our results were found identical to those reported, thus verifying the reliability of our methodology.

The following step in our procedure was to start all-electron calculations for the present system. More specifically, we employed the restricted second-order Møller−Plesset (MP2) perturbation theory for closed-shell systems (Cl_2, ClOH)[29] and the unrestricted Møller−Plesset (UMP2) theory with spin projection (PMP2/UMP2)[30,31] for open-shell systems (OH, ClClOH, Cl). The motivation of the spin-projection procedure arises from previous studies where the transition structures calculated at the unrestricted Hartree−Fock level were affected by a considerable amount of spin contamination, and as result the reaction barriers can be overestimated by up to 10 kcal/mol when correlation corrections are calculated by unrestricted Møller−Plesset perturbation theory. For simplicity reasons, in the rest of the paper we omit the U symbol when referring to UMP2 methodology. Thus, MP2 will simply denote MP2 or UMP2 depending on whether the number of electrons is even or odd, respectively. In the same manner, we replace the PMP2//UMP2 notation with PMP2. We initiated the calculations with the 6-31G(d) basis set and proceeded using the polarized MP2/6-311++G(d,p),[32] which was the starting point of our large-scale calculations. Then we proceeded with the polarized correlation-consistent cc-pVnZ[33,34] basis sets for $n = 2$ and 3, and finally we employed the augmented with diffuse functions aug-cc-pVDZ basis set. Pure d and f functions were used in the d and f shells; i.e., the d functions have five components and the f functions seven.

Due to computational time limitations, only the MP2 level of theory was examined in connection with the five basis sets mentioned above, and no other methodologies have been attempted. However, since the main purpose of the present work is the satisfactory description of the PES for the HO + Cl_2 reaction, and since no dramatic improvements are expected in the details of the determined structures for this particular purpose from going to a higher level of theory—as is also observed by Aloisio and Francisco[26] in the case of HCl···ClO and Cl_2···ClO complexes—we do not consider these limitations as a severe handicap in the present study. Similar effects were quoted in the theoretical study of hydrogen halide dimers, $(HX)_2$ (X = F through At).[35] There too, the small-scale calculations at the UMP2/6-31G* and UMP2/6-31** levels predicted quite correctly the $(HCl)_2$ and heavier hydrogen halide dimer structures, confirmed at the CCSD(T)/aug-cc-pVTZ level, while discrepancies appeared only in the results for $(HF)_2$ species.

Three optimized structures relevant to the title reaction were derived in the present study by performing all electron calculations with fully unconstrained geometry optimizations. We used a C1 point group symmetry for each species as the initial geometry of the optimization procedure, and we performed optimizations in redundant internal coordinates. The resulting point group symmetries with all basis sets employed are *D*8*h* for Cl_2 , *C*8*v* for OH, and *Cs* for ClOH and all ClClOH minimum-energy structures whereas the symmetry is *C*1 for the ClClOH saddle point. The optimized structures derived using the aug-cc-pVDZ basis set are shown in Figure 1, and the geometries, harmonic frequencies, and energetic parameters at all levels of calculations are summarized in Tables 1 and 2. The vibrational frequencies were calculated for each basis set to determine the nature of the stationary points and the zero-point-energy (ZPE) corrections. The most interesting configuration is structure **I**, which was determined to represent a transition-state configuration, linking reactants and products and reflecting the experimentally observed small activation energy barrier of the reaction. It possesses a nonplanar geometry verified using all five basis sets, with a dihedral angle near 70° and with both the constituent species Cl_2 and OH almost unchanged compared to their monomer structures. The O···Cl internuclear distance is found to be 1.895 Å, about 10% extended compared to the OCl bond distance in free HOCl. The calculated energy barrier heights must be overestimated, but the geometry of the transition state seems reasonable. The system passes through this configuration and by the gradual separation of the two Cl atoms reaches the minimum of the PES, HOCl···Cl, and proceeds further into the product valley. The nonplanar geometry of the ab initio determined transition-state configuration makes the present system quite analogous to the OH + CO reaction.[36] In that system the most probable pathway involves an interconversion between the cis- and trans-minima of HOCO over an isomerization barrier of nonplanar geometry similar to that

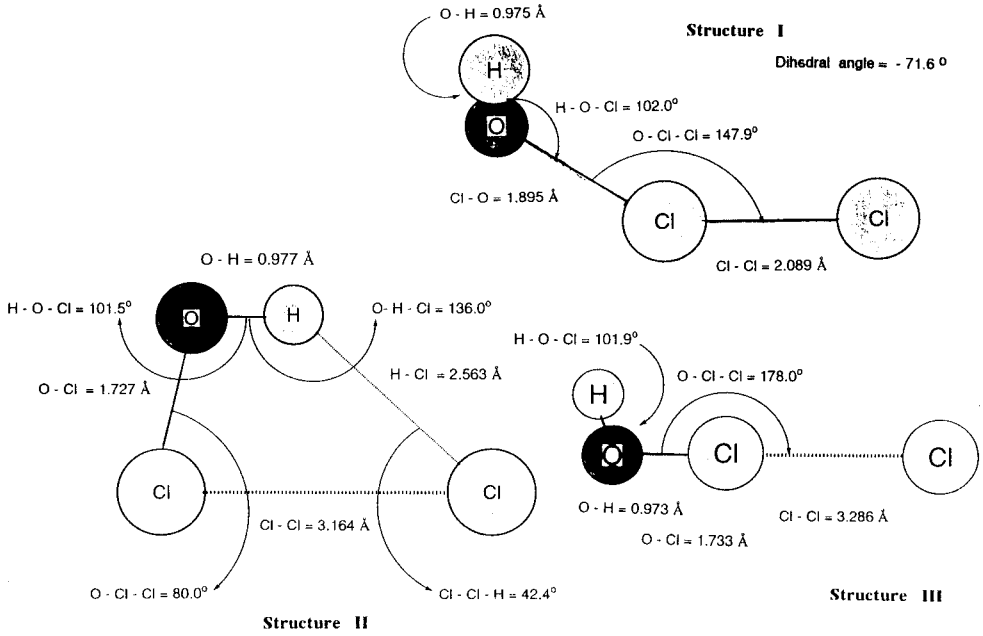

Figure 1. Optimized transition-state and minimum-energy structures of the HO + Cl_2 system at the MP2(full)/aug-cc-pVDZ level of theory.

of the present one, which leads through the cis-configuration into the H + CO_2 products.[37]

The other two structures, hereafter denoted as **II** and **III**, represent energy minima with significant binding energies with respect to reactants, which vary depending on the basis set used. Consistency in the binding energy results is observed in the values obtained from the two basis sets supplemented with diffuse functions, and these results are taken into account in the construction of the PES. Both structures present planar geometries and involve the triatomic HOCl group connected to the fourth atom, the second Cl atom. The interbond angle in the HOCl entity is found to be about 102°, the same as in the free HOCl molecule, and actually all geometrical parameters of the HOCl group in both tetratomic complexes under consideration fit well with the structural parameters of the free HOCl molecule.[38−41] Thus, both structures **II** and **III** should be characterized as HOCl···Cl complexes, and they must be important energy minima in the reverse Cl + HOCl reaction,[19] representing the attack of the HOCl molecule by the approaching Cl atom from either the H or the Cl end of HOCl. In structure **II**, the most stable one, the H···Cl distance was determined as 2.563 Å using the aug-cc-pVDZ basis set, comparable with the analogous H···Cl distance, 2.720 Å, found by Kollman et al.[42] for the hydrogen-bonded HCl dimer and consistent with the values determined in the recent studies of $(HX)_2$ species.[35] Hence, it certainly represents a hydrogen-bonded structure with a trapezoidal overall geometry. Structure **III** can be clearly characterized as a van der Waals complex with nearly collinear O−Cl···Cl atoms and a Cl···Cl distance of 3.286 Å in aug-cc-pVDZ, which compares well with the value 3.483 Å of the corresponding Cl···Cl van der Waals distance in the tetratomic ClCl···ClO complex.[26] The structural parameters from all basis sets agree well with each other, and also good consistency is observed in the isomerization energies between the two minimum-energy structures. The values from all basis sets are similar within 1.5 kJ mol^{-1}. The structural data along with the electronic energies and the resulting stabilization energies with respect to OH + Cl_2 reactants and the isomerization energies are summarized in Table 2. The vibrational harmonic frequencies are also given in Table 2, and there too a good overall agreement is obtained from all basis set calculations.

PES and Trajectory Calculations

Using the above information, our previously constructed global PES based on the Elgersma and Schatz formulation was accordingly modified to carry out the dynamics calculations. Briefly, the analytical functional structure of this potential has the form

$$V(R_{HO},R_{HCl},R_{HCl'},R_{OCl},R_{OCl'},R_{ClCl'}) = V_{LEPS}(R_{OCl},R_{OCl'},R_{ClCl'}) + V_M(R_{HO}) + V_{M^*}(R_{HCl}) + V_{M^*}(R_{HCl'}) + V_{HOCl}(R_{HO},R_{OCl},R_{HCl}) + V_{HOCl'}(R_{HO},R_{OCl'},R_{HCl'}) \quad (1)$$

Thus, it includes a LEPS switching term to describe the O−Cl−Cl′ interaction to transfer from reactants to products and a usual Morse potential, V_M, to account for the H−O bond. The two H−Cl and H−Cl′ interactions are approximated by two perturbed Morse potentials, V_{M^*} described by perturbed Morse parameters, D_{M^*}, β_{M^*}, R_{M^*}, optimized to fit the forces betweem H and Cl and between H and Cl′ atoms within the HOClCl′ transition state.

$$V_{M^*}(R) = D_{M^*}\{\exp[-2\beta_{M^*}(R_{HCl} - R_{M^*})] - 2\exp[-\beta_{M^*}(R_{HCl} - R_{M^*})]\} \quad (2)$$

Finally, a modified Sorbie−Murrell type three-body potential[43] for HOCl and HOCl′ is used, V_{HOCl} and $V_{HOCl'}$, to provide HOCl with a good approximation to the true quadratic force field.

$$V_{HOCl}(R_{HO},R_{OCl},R_{HCl}) = D^\circ_{HOCl}P(R_{HO},R_{OCl},R_{HCl})\,Q(R_{HO},R_{OCl},R_{HCl}) \quad (3)$$

with

$$P(R_{HO},R_{OCl},R_{HCl}) = 1 + \sum_{i=1}^{3} c_i S_i + \sum_{i=1}^{3} c_{ii} S_i^{\,2} + \sum_{j>i=1}^{3} c_{ij} S_i S_j \quad (4)$$

and

TABLE 1: Structural Parameters, Harmonic Frequencies, and Energetic Results for the Transition-State Configuration and Reactants and Products of the OH + Cl_2 Reaction[a]

Transition State

	6-31G(d)	6-311++G(d,p)	cc-pVDZ	aug-cc-pVDZ	cc-pVTZ
r(HO)	0.981	0.968	0.977	0.975	0.967
r(ClO)	1.877	1.862	1.864	1.895	1.889
r(ClCl)	2.091	2.095	2.115	2.088	2.045
∠(HOCl)	102.7	103.8	101.8	102.1	101.3
∠(OClCl)	148.5	147.2	148.9	147.9	148.4
ψ	−69.8	−70.0	68.5	−71.6	−70.2
frequencies	3692, 1048, 467, 351, 215, 742i	3828, 988, 482, 346, 214, 737i	3773, 1013, 457, 341, 216, 753i	3745, 980, 525, 354, 204, 639i	3812, 964, 555, 350, 207, 592i
E_{el}	−994.68659	−994.92656	−994.77661	−994.83700	−995.06971
ZPE corr	0.01316	0.01335	0.01321	0.01323	0.01341
ΔE[b]	29.9	36.3	35.7	16.3	18.6

Reactants

	r, ϑ	frequency	E_{el}	ZPE corr
		OH		
6-31G(d)	0.979	3721	−75.52144	0.00848
6-311++G(d,p)	0.968	3841	−75.60021	0.00875
cc-pVDZ	0.974	3794	−75.54633	0.00864
aug-cc-pVDZ	0.975	3769	−75.56950	0.00859
cc-pVTZ	0.966	3837	−75.63309	0.00874
		Cl_2		
6-31G(d)	2.018	541	−919.17656	0.00123
6-311++G(d,p)	2.039	547	−919.34020	0.00125
cc-pVDZ	2.030	547	−919.24389	0.00125
aug-cc-pVDZ	2.039	537	−919.27372	0.00122
cc-pVTZ	1.993	583	−919.44372	0.00133

Products

	r, ϑ	frequencies	E_{el}	ZPE corr
		HOCl[c]		
6-31G(d)	0.979, 1.717, 102.6	3698, 754, 1319	−535.15858	0.01314
6-311++G(d,p)	0.965, 1.714, 102.8	3838, 728, 1210	−535.31349	0.01316
cc-pVDZ	0.973, 1.729, 100.7	3787, 734, 1247	−535.21062	0.01314
aug-cc-pVDZ	0.974, 1.731, 101.9	3745, 742, 1254	−535.25407	0.01308
cc-pVTZ	0.965, 1.693, 101.9	3819, 774, 1277	−535.40403	0.01337
		Cl		
6-31G(d)			−459.55620	
6-311++G(d,p)			−459.63651	
cc-pVDZ			−459.58780	
aug-cc-pVDZ			−459.60001	
cc-pVTZ			−459.67760	

[a] Bond lengths in angstroms, bond angles in degrees, frequencies in cm^{-1}, and electronic energies and ZPE corrections in hartrees. [b] Energy difference with respect to the reactants. [c] Data in sequence refer to bond distances HO and OCl and bond angle HOCl, respectively.

$$Q(R_{HO},R_{OCl},R_{HCl}) = \prod_{i=1}^{3}[1 - \tanh(0.5\gamma_i S_i)] \qquad (5)$$

The displacement coordinates S_i in eqs 4 and 5 are given by $S_1 = R_{HO} - R^\circ_{HO}$, $S_2 = R_{OCl} - R^\circ_{OCl}$, or $S_2' = R_{OCl'} - R^\circ_{OCl}$, and $S_3 = R_{HCl} - R^\circ_{HCl}$ or $S_3' = R_{HCl'} - R^\circ_{HCl}$, where the R°_i distances represent the equilibrium reference frame distances of HOCl used by Murrell.[43]

The constructed surface produces a linear approximation to the transition-state configuration, located at 10.7 kJ mol^{-1} above the entrance valley at an O···Cl distance of 2.640 Å and a HOCl angle of 103°. Analogous collinear transition states have been considered in the study of the dynamics of other diatom−diatom systems such as the HO + HCl and HO + HBr reactions[44,45] also studied by quasiclassical dynamical calculations. The optimized surface also contains a considerable potential energy well of 37.8 kJ mol^{-1} representing the two close-lying minima **II** and **III**. Their geometries derived by the quantum calculations are located into the exit valley, so they are not well reproduced by the surface, but this discrepancy is not expected to be crucial since these two minima must be most critical in the reverse HOCl + Cl → HO + Cl_2[19] reaction. All parameters and characteristics of the surface are given in Table 3, and potential energy contours for the collinear approach of reactants are depicted in Figure 2 with the nonreactive OH bond fixed at the equilibrium distance. In addition, in Table 3 the aug-cc-pVDZ ab initio values for the stationary points are included in parentheses for comparison with the corresponding properties of the constructed surface. The deviations are whithin 10% between the quantum values and the constructed surface except for the location of the minimum along the Cl···Cl coordinate, which as mentioned above is not properly reproduced, and the energy barrier at the entrance of the reaction, which is clearly overestimated by the quantum calculations. However, although the accuracy of the present surface may not reach that of the Schatz surface for HO + H_2, the moderate deviations obtained indicate a good representation of the present system by the proposed surface, taking into account the size of the system and the spreading of the ab initio calculations.

TABLE 2: Structural Parameters, Harmonic Frequencies, and Energetic Results for the Two Optimized Minimum-Energy Structures of the HOClCl System

	6-31G(d)	6-311++G(d,p)	cc-pVDZ	aug-cc-pVDZ	cc-pVTZ
			Structure II		
HO	0.979	0.968	0.974	0.977	0.968
ClO	1.716	1.713	1.727	1.727	1.691
ClCl′	4.293	3.925	3.168	3.164	3.187
Cl′H	2.599	2.585	2.578	2.563	2.568
ClHCl′	129.0	112.0	95.6	83.9	84.3
HOCl	102.6	102.3	100.4	101.5	101.3
Cl′HO	178.9	163.5	160.3	135.9	136.5
frequencies	3701, 1339, 755, 152, 95, 33	3818, 1223, 730, 224, 89,14	3772, 1266, 736, 204, 99, 23	3694, 1280, 745, 206, 112, 43	3761, 1302, 774, 236, 115, 20
E_{el}[a]	−994.71748	−994.95338	−994.80140	−994.85867	−995.08557
ZPE corr	0.01384	0.01389	0.01389	0.01385	0.01414
DE[b]	52.2	36.1	30.0	41.4	22.7
			Structure III		
HO	0.979	0.965	0.973	0.974	0.965
ClO	1.718	1.716	1.730	1.733	1.695
ClCl′	3.522	3.477	3.502	3.286	3.272
HOCl	102.6	102.9	100.7	101.9	101.9
OClCl′	179.7	177.3	179.5	178.0	179.0
frequencies	3699, 1318, 752, 47, 44,23	3839, 1207, 726, 53, 50, 39	3788, 1244, 731, 47, 44, 26	3747, 1250, 736, 67, 63, 46	3820, 1274, 769, 54, 53, 40
E_{el}[a]	−994.71584	−994.95206	−994.79956	−994.85644	−995.08325
ZPE corr	0.01340	0.01347	0.01340	0.01346	0.01369
ΔE[b]	46.8	30.6	24.5	34.7	16.9
ΔE_{is}[c]	5.4	5.5	5.5	6.7	5.8

[a] Bond lengths in angstroms, bond angles in degrees, frequencies in cm^{-1}, and electronic energies and ZPE corrections, in hartrees. [b] Binding energies with respect to reactants OH and Cl_2, kJ mol^{-1}, calculated at the same level of theory. [c] Energy difference between the two minimum-energy structures kJ mol^{-1}.

TABLE 3: Molecular Parameters and Dynamical Characteristics of the PES Constructed

parameter	HO	Cl_2	OCl	HCl
R_e,[a] Å	0.965	1.999	1.571	1.275
β_e,[a] $Å^{-1}$	2.295	2.008	2.290	
D_e,[a] kJ mol^{-1}	441.9	242.8	270.5	445.5
ν,[a] cm^{-1}	3735	565		
ν,[b] cm^{-1}	3617		739	
ν,[b] cm^{-1} (HOCl bending mode)	1242			
B_e,[a] cm^{-1}	18.87	0.244		
R_{M^*},[c] Å				2.202
β_{M^*},[c] $Å^{-1}$				2.012
D_{M^*},[c] kJ mol^{-1}				36.5
Sato[d]		0.102	0.648	
$D°$ [e](HOCl), kJ mol^{-1}	64.45			
$R°$,[e] Å	0.965		1.690	2.119
c_i,[e] $Å^{-1}$	0.609		0.490	0.511
c_{ii},[e] $Å^{-2}$	0.030		0.051	0.089
c_{ij}[e] (HO,OCl), $Å^{-2}$	0.013			
c_{ij}[e] (HO,HCl) $Å^{-2}$	0.072			
c_{ij}[e] (HO,HCl), $Å^{-2}$	0.037			
γ_i,[e] $Å^{-1}$	4.007		1.490	1.048
E_b,[f] kJ mol^{-1}	10.7 (16.3)			
R_b,[f] Å	0.965 (0.975)	2.020 (2.088)	2.640 (1.895)	
E_w,[f] kJ mol^{-1}	37.8 (41.4)			
R_w,[f] Å	0.965 (0.977)	2.180 (3.164)	1.680 (1.727)	
ΔD_o,[g]/kJ mol^{-1}	6.8			

[a] Diatomic spectroscopic constants taken or calculated from ref 55. [b] Referring to properties within the HOCl molecule from ref 38b. [c] Perturbed Morse parameters. [d] Adjusted Sato values. [e] Original and modified Murrell parameters. [f] Barrier height and location, potential well, and location of the constructed surface. The values in parentheses are the aug-cc-pVDZ results also included here for comparison. [g] Accepted value for the endoergicity of the reaction from ref 38a.

Quasiclassical three-dimensional trajectory calculations were performed by using a suitably modified version of the Mercury program[46] in which the potential energy function of eqs 1−5 and its partial derivatives have been incorporated. The standard

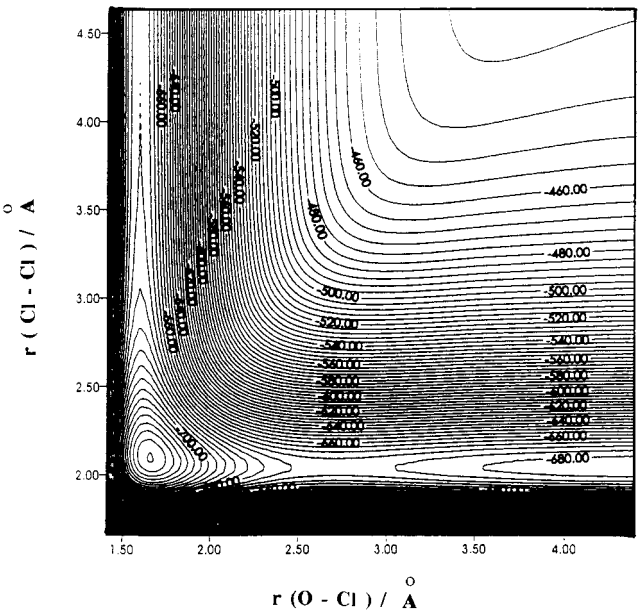

Figure 2. Potential energy contours spaced by 4 kJ/mol for the collinear approach of the reactants, calculated by fixing the OH distance at the spectroscopic equilibrium bond value and the HOCl angle to 102.5°.

random selection of initial conditions[47] were used. A total of 30 000 trajectories were run at each collision energy, E_T, for a series of 12 values of E_T from 4 to 100 kJ/mol and a range of b_{max} values from 2.5 to 2.8 Å with increasing E_T. The large number of trajectories was necessary to obtain good statistics due to the low reactivity especially in the low-energy regime. The initial conditions were assumed to be the zero vibrational level for each reactant, $v = 0$, and the rotational numbers $J = 2$ for OH and $J = 20$ for Cl_2, which are the most populated rotational levels for these species at 298 K. Next, the selectivity of initial reactant internal energy upon reactivity was studied at three different values of the collision energy, 12, 25, and 38

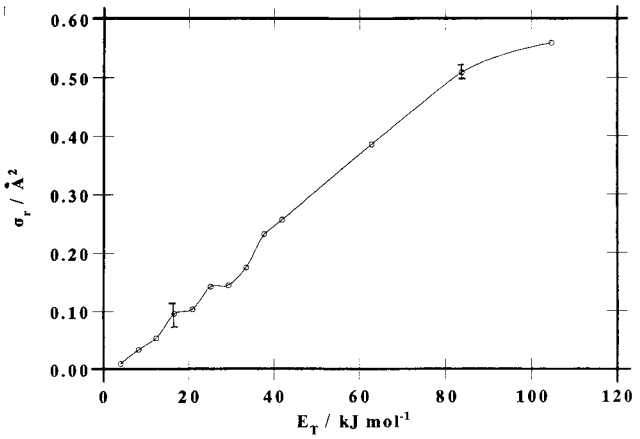

Figure 3. Reactive cross section vs initial collision energy calculated with zero initial vibrational energy and the most probable reactant rotational energy at 298 K. The error bars indicate the statistical errors calculated according to ref 56.

TABLE 4: Comparison of Experimental and Theoretical Rate Constants at 298 K in Units of $\times 10^{-14}$ cm^3 molecule^{-1} s^{-1}

k_{exp}	6.70 ± 0.72,[a] 6.8 ± 1.0,[b] 5.5 ± 0.3,[c] 7.4[d]
k_{theor}	7.1

[a] Reference 14. [b] Reference 15. [c] Reference 10. [d] Reference 11.

kJ mol^{-1}, for a number of internal states of the reactants. A series of calculations were performed for each of the following quantum states of reactants, v_{OH} = 0, 1, 2, and 5, v_{Cl_2} = 0, 1, 2, and 5, J_{OH} = 0, 1, 2, and 5, and J_{Cl_2} = 0, 10, 20, and 30, keeping zero all the other quantum numbers for both reactants in each calculation. Finally, the partitioning of the total available energy among products at E_T = 12 and 38 kJ mol^{-1} is investigated for a series of values of reactant vibrational excitation under the same initial conditions.

Trajectory Results

The reactive cross section calculated from

$$\sigma_r(E_T) = \pi b_{max}(E_T)[N_r(E_T)/N_{tot}] \qquad (6)$$

is depicted as a function of initial collision energy in Figure 3. A monotonic increase is observed up to high collision energy values with saturation reachable only at high initial energies as the system displays the typical behavior of a reaction with an energy barrier at the entrance valley. The corresponding reaction coefficient at 298 K is calculated by the standard formula

$$k(E_T) = g\left[\frac{8}{(k_B T)^3 \pi \mu}\right]^{1/2} \int_{E_o}^{\infty} E_T \sigma_r(E_T) e^{-E_T/k_B T}\, dE_T \qquad (7)$$

trough a polynomial fitting of the appropriate $\sigma_r(E_T)$ vs E_T curve. The multiple surface factor g is included to ensure reactive collisions are counted only on the lowest adiabatic electronic PES and is taken equal to $1/[1 + \exp(-E/T)]$, where E = 181 K is the splitting between the $^2\Pi_{3/2}$ and $^2\Pi_{1/2}$ levels of OH.[44,45] The calculated value is compared to various experimental results in Table 4, where a satisfactory agreement is observed between the theoretical rate constant and the experimental measurements.

The main purpose of the present study is focused on the investigation of the selectivity of reactant internal energy upon the reactivity of the system. Figures 4 and 5 show the influence of vibrational and rotational excitation at three initial collision energy values, 12, 25, and 38 kJ mol^{-1}. We observe a

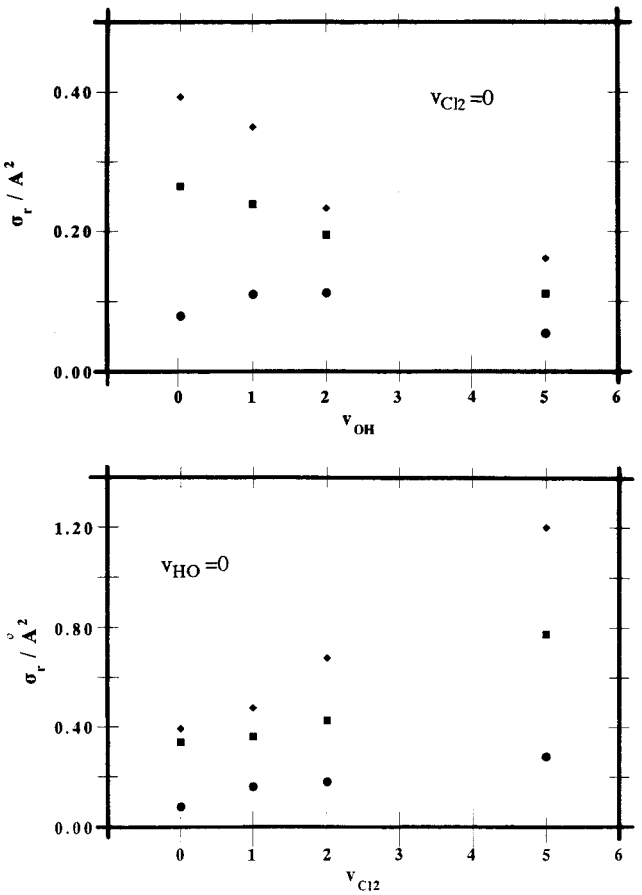

Figure 4. Reactive cross sections vs reactant vibrational state and zero initial rotational energy calculated at three values of initial collision energy from the bottom to the top, 12, 25, and 38 kJ mol^{-1}.

considerable enhancement of the reactive cross section with an increase in the vibration of the breaking ClCl bond, and the effect becomes quite prominent when coupled with an increase in the initial translational energy of the collision. The exactly opposite effect is observed when the OH reactant is vibrationally excited for 25 and 38 kJ mol^{-1} of collision energy. At 12 kJ mol^{-1} an increase is obtained in σ_r at low v_{OH} values, which again declines at higher values of OH vibrational quantum numbers. Thus, regarding the vibrational energy dependence, the general propensity rule that was manifested in other diatom−diatom cases appears to apply here too, namely, that an increase in the reactive bond vibration significantly promotes the rate of the reaction, while exciting the nonbreaking bond produces an opposite effect. Quite analogous effects have been observed in studies of other diatom−diatom systems, for example, the BO + H_2 → HBO + H,[48] NH + NO → NNO + H[49], and CN + H_2 → HCN + H[50] reactions, where an increase in the reactive bond vibration was found to enhance the reactivity considerably, while an increase in the spectator bond vibrational excitation resulted in a severe decline of the reaction probability. The promoting effect of the breaking bond vibration on reactivity was also observed in the studies of the OH + H_2 → H_2O + H[51−53] reaction, and it is somehow expected because the vibrational excitation weakens the bond. However, in the investigation of the latter system and in other studies of CN + H_2 → HCN + H,[54] the inhibitive effect of the spectator bond vibration was found much milder or even negligible. It is possible that some kind of correlation between the mass of the spectator atom of the spectator bond and the amount of inhibition induced may operate, but many more data on this feature are

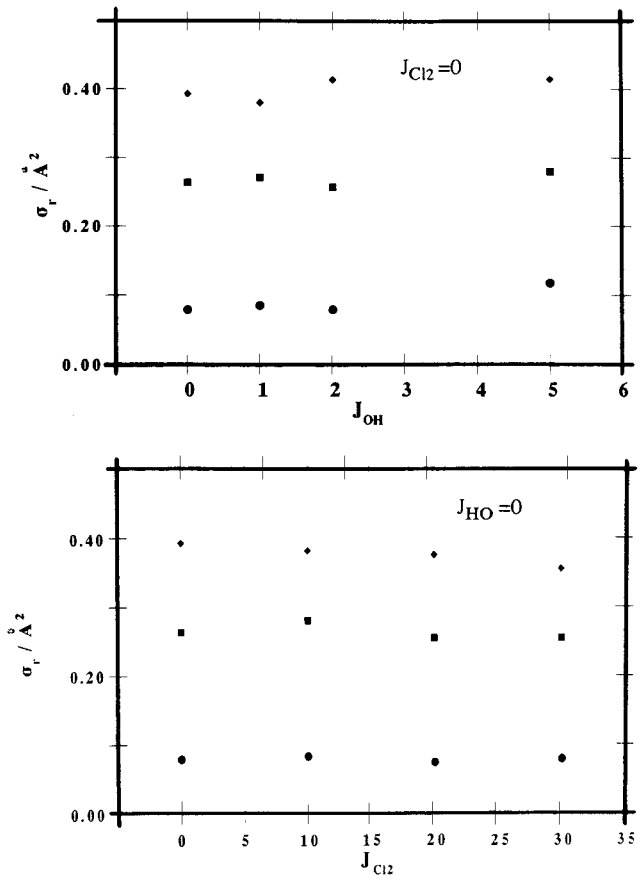

Figure 5. Reactive cross sections vs reactant rotational state and zero initial vibrational energy calculated at three values of initial collision energy from the bottom to the top, 12, 25, and 38 kJ mol^{-1}.

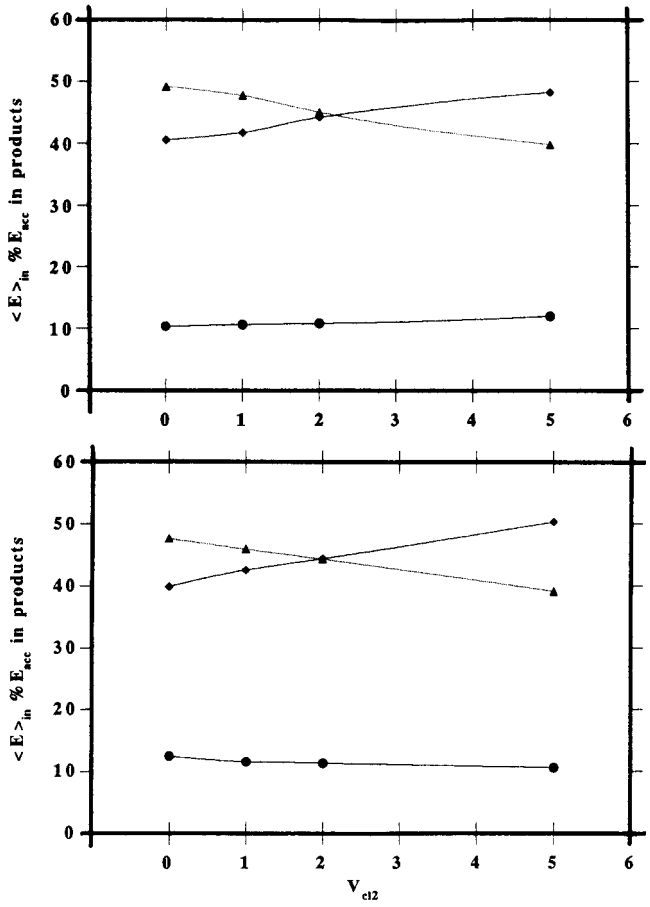

Figure 6. Percentage of available energy going into product rotation (circles), vibration (squares), and translation (triangles) for two values of initial collision energy, 12 (top) and 38 (bottom) kJ mol^{-1} vs HO vibration, $J_{OH} = 0$, $v_{Cl_2} = 0$, $J_{Cl_2} = 0$.

required to confirm this argument. The prohibitive action of the nonbreaking bond vibration combined with the corresponding promoting effect of the reactive bond has been discussed in detail for both the BO + H_2 → HBO + H[48] and NH + NO → NNO + H[49] reactions, and various qualitative pictures were used to describe these effects. The inhibition in these cases was described as the result of the efficient rebound of the reactive H_2 or NH by the vibrating, much heavier BO or NO molecule. Another picture which could be considered complementary to the kinematic one, especially at the low-energy region, describes the inhibition as a result of the enlarging distance of the vibrating, nonbreaking bond and the increasing importance of repulsive configurations that make rebounding trajectories significant. It is difficult to classify the OH + Cl_2 system to one or the other of the above-mentioned prototypes considering the much heavier reduced mass of the breaking bond compared to the spectator in the present case. Here, the approaching OH radical combines linearly with the vibrating Cl_2 molecule in the transition-state region, and the increasing vibrational content of the chlorine molecule tends to expand the ClCl bond distance and facilitate the rebound of the HOCl entity with most of the translational energy conserved. Thus, Cl_2 vibrational excitation promotes the reactivity, while the OH vibration proves unable to help in surmounting the barrier of the reaction.

Evidence of normal-mode separability is also obtained from the product energy partitioning variation as the reactant vibrational energy is modified. Figures 6 and 7 present the disposal of available energy among reaction products at two values of the collision energy, 12 and 25 kJ mol^{-1}. The general pattern is the same at both energies, but the tendencies observed regarding the selectivity of the initial vibration of either the reactive or the spectator bond are quite interesting. When no reactant vibrational excitation is present, the distribution of available energy between product vibration and translation is approximately even with a slight excess of translation. As vibrational energy is put into the breaking bond, the percentage of product translation slowly declines with a corresponding moderate increase in product vibration. The same effect has been obtained in the BO + H_2 → HBO + H reaction[48] when an increase in the vibrational energy content in any of the two reactants is observed. However, the product vibrational energy increase becomes quite pronounced for the present system when the vibration of the nonbreaking bond is increased, reflecting the much larger vibrational quantum associated with OH vibration compared to Cl_2. As a result a striking drop in the percentage of product translational energy is obtained with a corresponding impressive increase in product vibration, leading to the conclusion that the major part of OH initial vibration remains confined in the stretching mode of this particular bond within the HOCl product. Thus, the assumption of the spectator role of OH bond and the adiabatic behavior of the collision with respect to the OH vibration are clearly manifested.

The influence of initial rotation is much weaker as shown in Figure 5 and leads to a negligible overall effect on reaction probability with initial Cl_2 rotational excitation and a very feeble increase with initial OH rotation. Also the percentage of accessible energy transferred into product rotation remains unaltered, independent of the initial translational or vibrational state of the reactants.

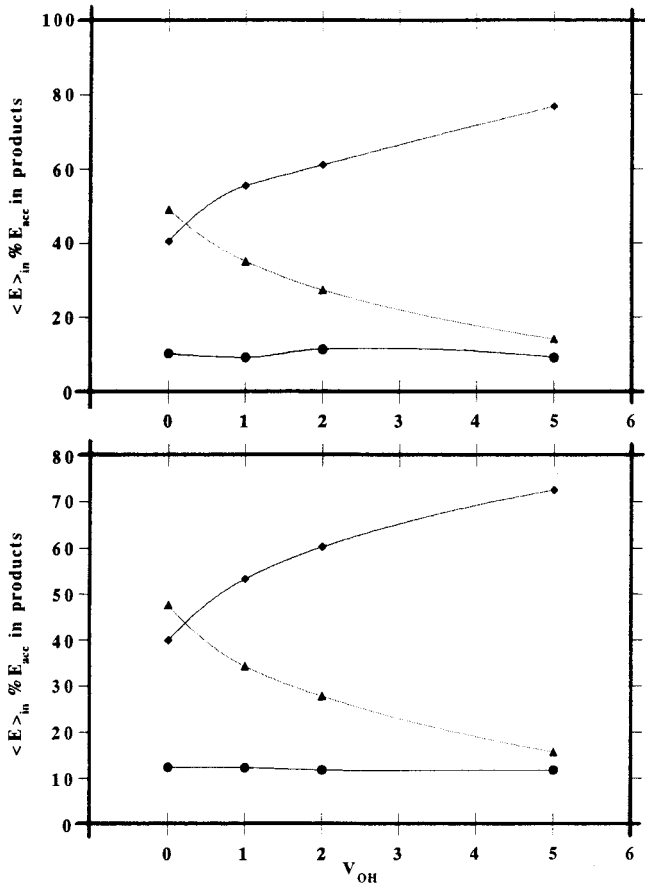

Figure 7. Percentage of available energy going into product rotation (circles), vibration (squares), and translation (triangles) for two values of initial collision energy, 12 (top) and 38 (bottom) kJ mol^{-1} vs Cl_2 vibration, $J_{Cl_2} = 0$, $v_{OH} = 0$, $J_{OH} = 0$.

We conclude that the present calculations appear to satisfactorily describe the dynamics of the OH + Cl_2 reaction apart from the uncertainty associated with the absence of the ZPE constraint in the QCT procedure applied. Due to the low reactivity of the system, especially in the low-energy region, no attempts have been made to examine the individual trajectories and discard those violating the ZPE rule. We believe that we can accept the validity of the present quasiclassical calculations considering the adiabaticity associated with the vibrational excitation of the OH bond and thus reasonably assuming that the excess energy over the endothermicity of the reaction covers the low zero-point energies of O−Cl bond stretching and HOCl bending modes without violating the zero- point energy principle.

Summary

The selectivity of reactant rotational and vibrational energy upon reactive cross sections for the reaction OH + Cl_2 → HOCl + Cl has been investigated in detail by performing QCT calculations on a six-dimensional, analytical PES. The construction of the PES was based on an ab initio quantum mechanical study of the HOClCl system at the MP2(full) level of theory, using the 6-31G(d), 6-311++G(d,p), cc-pVnZ, $n = 2$, 3, and aug-cc-pVnZ basis sets. A nonplanar transition-state structure and two planar minimum-energy structures were determined relevant to the present reaction.

Extended three-dimensional QCT calculations have been performed for collision energy values up to 100 kJ mol^{-1}, which have allowed the proper characterization of the dependence of the reactive cross section on collision energy and the calculation of the rate coefficient at 298 K, which compares well with the experimental measurements. The results demonstrate the significant promotion of reactivity with increasing collision energy. Regarding the influence of internal energy, an inhibition of the reactivity is observed when the initial OH vibration increases, especially at high collision energies. On the other hand, the Cl_2 vibrational excitation leads to a clear enhancement of the reaction probability consistent with similar effects observed in other diatom−diatom reactions. Finally, the disposal of total available energy vs reactant internal energy is studied, and it is found that the percentage of the available energy channeled into product vibration increases with reactant vibration, an effect that becomes quite prominent when initial OH vibration is concerned and which demonstrates the adiabatic character of the collision and the spectator role of OH.

Acknowledgment. Computer services provided by the Computer Center of the University of Ioannina, the Laboratory of Applied Quantum Chemistry of Aristotle University of Thessaloniki, and the Cineca Supercomputer Center of Bologna, Italy, are gratefully acknowledged.

References and Notes

(1) Clary, D. C. *J. Phys. Chem.* **1994**, *98*, 10678 and references therein.
(2) Wang, D.; Bowman, J. M. In *Advances in Molecular Vibrations and Collisions Dynamics*; Bowman, J. M., Ed.; JAI Press: Greenwich, CT, 1994.
(3) Schatz, G. C. *J. Phys. Chem.* **1995**, *99*, 516 and references therein.
(4) Bowman, J. M.; Schatz, G. C. *Annu. Rev. Phys. Chem.* **1995**, *46*, 169.
(5) Alagia, M.; Balucani, N.; Casavecchia, P.; Strange, D.; Volpi, G. G. *J. Chem. Soc., Faraday Trans.* **1995**, *91*, 575 and references therein.
(6) *J. Chem. Soc., Faraday Trans.* **1997**, *93*, Special Issue on the "Quantum Theory of Chemical Reactions".
(7) Clary, D. C. *Science* **1998**, *279*, 1817.
(8) Zare, R. N. *Science* **1998**, *279*, 1889.
(9) Parrish, D. D.; Herschbach, D. R. *J. Am. Chem. Soc.* **1973**, *95*, 6136. Herschbach, D. R. *Faraday Discuss. Chem. Soc.* **1973**, *55*, 233.
(10) Leu, M. T.; Lin, C. L. *Geophys. Res. Lett.* **1979**, *6*, 425.
(11) Ravishankara, A. R.; Eisele, F. L.; Wine, P. H. *J. Chem. Phys.* **1983**, *78*, 1140.
(12) Poulet, G.; Leverdet, G.; LeBras, G. *Chem. Phys. Lett.* **1983**, *94*, 129.
(13) Jenkin, M. E.; Chemitshaw, K. C.; Cox, R. A. *J. Chem. Soc., Faraday Trans.* 2 **1984**, *80*, 1633.
(14) (a) Loewenstein, L. M.; Anderson, J. G. *J. Phys. Chem.* **1984**, *88*, 6277. (b) Loewenstein, L. M.; Anderson, J. G. *J. Phys. Chem.* **1985**, *89*, 5371.
(15) Boudaghians, R. B.; Hall, I. W.; Wayne, R. P. *J. Chem. Soc., Faraday Trans. 2* **1987**, *83*, 529.
(16) Veltman, I.; Durkin, A.; Smith, D. J.; Grice, R. *Mol. Phys.* **1980**, *40*, 213.
(17) Loewenstein, L. M.; Anderson, J. G. *J. Phys. Chem.* **1987**, *91*, 2993.
(18) Mohr, S.; Goonan, K. M.; Wells, D. D.; Grice, R. *J. Phys. Chem. A* **1997**, *101*, 9699.
(19) (a) Cook, J. E. L.; Ennis, C. A.; Leck, T. J.; Birks, J. W. *J. Chem. Phys.* **1981**, *74*, 545. (b) Cook, J. E. L.; Ennis, C. A.; Leck, T. J.; Birks, J. W. **1981**, *75*, 497.
(20) Kosmas, A. M.; Drougas, E. *Chem. Phys.* **1997**, *229*, 233.
(21) (a) Sun, Q.; Bowman, J. M. *J. Chem. Phys.* **1990**, *92*, 5201. (b) Wang, D.; Bowman, J. M. *J. Chem. Phys.* **1992**, *96*, 8906.
(22) Schatz, G. C.; Elgersma, H. *Chem. Phys. Lett.* **1980**, *73*, 21.
(23) (a) Brooks, A. N.; Clary, D. C. *J. Chem. Phys.* **1989**, *92*, 1990. (b) Clary, D. C. *J. Chem. Phys.* **1991**, *95*, 7298.
(24) Rohrbacher, A.; Williams, J.; Janda, K. C.; Cybulski, S. M.; Burcl, R.; Szczesniak, M. M.; Chalasinski, G.; Halberstadt, N. *J. Chem. Phys.* **1997**, *106*, 2685 and references therein.
(25) Resende, S. M.; De Almeida, W. B. *Mol. Phys.* **1997**, *91*, 635.
(26) Aloisio, S.; Francisco, J. S. *Chem. Phys.* **1997**, *219*, 201.
(27) (a) Møller, C.; Plesset, M. S. *Phys. Rev.* **1934**, *46*, 618. (b) Frisch, M. J.; Head- Gordon, M.; Pople, J. A. *J. Chem. Phys.* **1990**, *141*, 189.
(28) Frisch, M. J.; Trucks, G. W.; Schlegel, H. B.; Gill, P. M. W.; Johnson, B. G.; Robb, M. A.; Cheeseman, J. R.; Keith, T. A.; Peterson, G. A.; Montgomery, J. A.; Raghavachari, K.; Al-Laham, M. A.; Zakrzewsky, V. G.; Ortiz, J. V.; Foresman, J. B.; Gioslowski, J.; Stefanov, B. B.;

Nanayakkara, A.; Challacombe, M.; Peng, C. Y.; Ayala, P. Y.; Cheng, W.; Wong, M. W.; Andres, J. L.; Replogle, E. S.; Gomperts, R.; Martin, R. L.; Fox, D. J.; Binkley, J. S.; DeFrees, D. J.; Baker, J.; Stewart, J. P.; Head-Gordon, M.; Gonzalez, C.; Pople, J. A. *GAUSSIAN* 94; Gaussian, Inc.: Pittsburgh, PA, 1995.

(29) Hehre, W. J.; Radom, L.; Schleyer, P. V. R.; Pople, J. A. *Ab Initio Molecular Orbital Theory*, Wiley: New York, 1986.

(30) (a) Soca, C.; Schlegel, H. B. *Int. J. Quantum Chem.* **1986**, *29*, 1001. (b) Soca, C.; Schlegel, H. B. *Ibid*. **1987**, *30*, 155.

(31) (a) Soca, C.; Schlegel, H. B. *Int. J. Quantum Chem. Symp*. **1987**, *21*, 267. (b) Gonzalez, C.; Soca, C.; Schlegel, H. B. *J. Phys. Chem.* **1989**, *93*, 2435.

(32) (a) Krishnan, R.; Binkley, J. S.; Seegar, R.; Pople, J. A. *J. Chem. Phys*. **1980**, *72*, 650. (b) McLean, A. D.; Chandler, G. S. *J. Chem. Phys*. **1980**, *72*, 5639.

(33) Dunning, Jr., T. H. *J. Chem. Phys*. **1989**, *90*, 1007.

(34) (a) Woon, D. E.; Dunning, Jr., T. H. *J. Chem. Phys*. **1993**, *98*, 1358. (b) Peterson, K. A.; Kendall, R. A.; Dunning, T. H., Jr. *J. Chem. Phys*. **1993**, *99*, 9790. (c) Davidson, E. R. *Chem. Phys. Lett.* **1996**, *220*, 514.

(35) Burda, J. V.; Hobza, P.; Zahradnik, R. *Chem. Phys. Lett.* **1998**, *288*, 20.

(36) Kudla, K.; Schatz, G. C.; Wagner, A. F. *J. Chem. Phys.* **1991**, *95*, 1635.

(37) Bradley, K. S.; Schatz, G. C. *J. Chem. Phys*. **1997**, *106*, 8464.

(38) (a) Hirsch, G.; Bruna, P. J.; Peyerimhoff, S. D.; Buenker, R. *J. Chem. Phys. Lett.* **1977**, *52*, 442. (b) Murrell, J. N.; Carter, S.; Mills, I. M.; Guest, M. F. *Mol. Phys.* **1979**, *37*, 1199.

(39) Lee, T. J. *J. Phys. Chem*. **1994**, *98*, 3697.

(40) Escribano, R. M.; Di Lonardo, G.; Fusina, L. *Chem. Phys. Lett.* **1996**, *259*, 614.

(41) (a) Koput, J.; Peterson, K. A. *Chem. Phys. Lett.* **1998**, *283*, 139. (b) Skokov, S.; Peterson, K. A.; Bowman, J. M. *J. Chem. Phys*. **1998**, *109*, 2662.

(42) Kollmann, P.; McKelvey, J.; Johansson, A.; Rothenberg, S. *J. Am. Chem. Soc.* **1975**, *97*, 955.

(43) Murrell, J. N.; Carter, S.; Farantos, S. C.; Huxley, P.; Varandas, A. C. J. *Molecular Potential Energy Functions*; Wiley: New York, 1984.

(44) Clary, D. C.; G. Nyman, G.; Hernandez, R. *J. Chem. Phys.* **1994**, *101*, 3704.

(45) Nizamov, B.; Setser, D. W.; Wang, H.; Pesiherbe, G. H.; Hase, W. H. *J. Chem. Phys.* **1996**, *105*, 9897.

(46) Hase, W. L. *QCPE* **1983**, *3*, 453.

(47) Duchovic, R. J.; Hase, W. L. *J. Chem. Phys.* **1985**, *82*, 3603.

(48) Sogas, J.; Alberti, M.; Gimenez, X.; Sayos, R.; Aguilar, A. *J. Phys. Chem. A* **1997**, *101*, 8877.

(49) Szichman, H.; Baer, M. J. *J. Chem. Phys.* **1996**, *105*, 10380.

(50) Zhu, W.; Zhang, J. Z. H.; Zhang, Y. C.; Zhang, Y. B.; Zhan, L. X.; Zhang, S. L.; Zhang, D. H. *J. Chem. Phys*. **1998**, *108*, 3509.

(51) Sun, Q.; Bowman, J. M. *J. Chem. Phys.* **1990**, *92*, 5201.

(52) Clary, D. C. *J. Chem. Phys.* **1992**, *96*, 3656.

(53) Balakrishnan, N.; Billing, G. D. *Chem. Phys.* **1994**, *189*, 499.

(54) Takayanagi, T.; Schatz, G. C. *J. Chem. Phys.* **1997**, *106*, 3227.

(55) Huber, K. P.; Herzberg, G. *Molecular Spectra and Molecular Structure*, *Constants of Diatomic Molecules*; van Nostrand Reinhold: New York, 1979.

(56) Raff, L. M.; Thomson, D. L. In *Theory of Chemical Reaction Dynamics*; Baer, M., Eds.; CRC Press: Boca Raton, FL, Vol. 3, 1985; Chapter.